

Radical reactions in the cold microwave plasma of atomized gases studied by continuous ESR flow technique

A. TKÁČ

*Department of Physical Chemistry, Faculty of Chemical Technology,
Slovak Technical University, CS-81237 Bratislava*

Received 18 June 1990

Dedicated to Professor L. Valko, DrSc., in honour of his 60th birthday

Diatomic gases of H_2 , N_2 , O_2 under reduced pressure and volatilized molecules of H_2O , D_2O , H_2O_2 , NH_3 , are effectively dissociated to their atoms, when they are exposed to microwave radiation of the frequency 2450 MHz. The formed paramagnetic species $H\cdot$, $D\cdot$, $\cdot\dot{N}$, $\cdot O$ are proved directly in the cold plasma by means of the identified ESR spectra. At constant power of the microwave transmitter (5 to 100 W) the highest spin concentration of atomized gases 2×10^{16} — 3×10^{16} spin cm^{-3} is reached in the vacuum interval of 100 up to 200 Pa. With increased pressure the atomized species gradually disappear in the consequence of recombination. In the homogeneous magnetic field of the ESR spectrometer using the TE_{102} mode cavity in the flowing cold plasma the secondary products of radical recombination as $HO\cdot$, $HOO\cdot$, $DO\cdot$ or $DOO\cdot$ were under the detectable sensitivity level. Nevertheless, their presence and the effect of the applied magnetic field on gas phase radical reactions were ascertained by introducing the spin-trapping technique transforming the primary instable radicals of the plasma to stable nitroso spin-adducts of DMPO (5,5-dimethyl-1-pyrroline *N*-oxide). The concentration relation between the highly reactive $HO\cdot$ and $HOO\cdot$ radicals as products of the reaction $\cdot O + HOH \rightarrow 2 HO\cdot$ was measured after freezing the radicals from the flowing plasma on the internal cryostat situated in the ESR cell and cooled with liquid nitrogen.

Elaborating a cross-flow experimental arrangement, the kinetics of the rapid reactions between the colliding atomized gases with different molecules when introduced into the ESR cell from the opposite direction to the plasma flow were observed. The reactivity of atomized oxygen with solid targets was measured directly in the ESR cavity. In this way the one-electron transfer from the chelated transition metal cobalt(II) $3d^7$ to atomized oxygen forming the complex $Co^{3+}O\cdot^-$ was proved. Atomized oxygen can initiate surface cross-linking after its addition to a double bond in contact with exposed films of natural rubber or polyisoprene.

Диатомные газы H_2 , N_2 , O_2 в пониженном давлении и летучие молекулы H_2O , D_2O , H_2O_2 , NH_3 диссоциированы в атомы, если подвергнуты микроволновой радиации в частоте 2450 МГц. Возникнувшие

парамагнитные частицы $\text{H}\cdot$, $\text{D}\cdot$, $\cdot\dot{\text{N}}\cdot$, $\cdot\text{O}\cdot$, были прямо доказаны в холодной плазме методом ЭСР-спектроскопии. При постоянной микроволновой радиации (5—100 В) максимальная спиновая концентрация атомизированных газов 2×10^{16} — 3×10^{16} спин см^{-3} была достигнута в интервале давления 100—200 Па. С повышением давления количество атомизированных соединений понижалось в настоянии рекомбинации. В однородном магнитном поле ЭСР-спектрометра и при использовании TE_{102} -резонансной полости в текущей холодной плазме была концентрация вторичных продуктов радикальной рекомбинации, как $\text{HO}\cdot$, $\text{HOO}\cdot$, $\text{DO}\cdot$ или $\text{DOO}\cdot$ ниже детектированного уровня. Однако, их присутствие и влияние использованного магнитного поля на радикальные реакции в газовой фазе, были доказаны введением техники спиновой ловушки трансформированием первичных нестабильных радикалов плазмы в стабильные нитроксидные спин-адукты ДМПО (5,5'-диметил-1-пирролин-*N*-оксида). Взаимоотношение концентраций между более реактивными $\text{HO}\cdot$ и $\text{HOO}\cdot$ радикалами, как продуктами реакции $\cdot\text{O}\cdot + \text{NOH} \rightarrow 2 \text{HO}\cdot$ были измерены после вымораживания радикалов из текущей плазмы криостатом охлаждаемым жидким азотом.

Была использована сложная аппаратура, где исследовались кинетики скорых реакций между атомизированными газами и различными молекулами введенными в ЭСР-спектрометр против текущей плазме. Реактивность атомизированного кислорода с жесткими соединениями была исследована прямо в ЭСР-резонансной полости. Этим методом был доказан одно-электронный перенос из хелатного металла $\text{Co}(\text{II}) 3d^7$ на атомизированный кислород за возникновения комплекса $\text{Co}^{3+}\text{O}\cdot^-$. Атомизированный кислород может инициировать поверхностные поперечные связи после его присоединения на двойную связь в контакте с подвергнутым фильмом природной резины или полиизопрена.

From the time ESR was introduced for direct proof of paramagnetic species, many comprehensive papers [1—5] have dealt with the theoretical and experimental background of radical gas phase chemistry. The interest to solve different practical problems applying the well elaborated basic theory [6—11] permanently increases, in spite of the fact that the detection of paramagnetic species in gas phase is limited only to atoms ($\text{H}\cdot$, $\text{D}\cdot$, $\cdot\text{O}\cdot$, $\cdot\dot{\text{N}}\cdot$, $\text{F}\cdot$, $\text{Cl}\cdot$, $\text{Br}\cdot$, $\cdot\text{I}\cdot$) and to diatomic ($\text{HO}\cdot$, $\cdot\text{SO}\cdot$, $\text{NO}\cdot$, $\cdot\text{O}_2\cdot$) or to linear triatomic free radicals ($\text{HOO}\cdot$, $\text{NO}_2\cdot$, $\text{NF}_2\cdot$, $\text{N}_3\cdot$). The sensitivity of ESR to detect multiatomic radicals, namely in gas phase, decreases as a consequence of strong coupling of their rotational angular moment (K) to the electron spin (S) and orbital (L) moment, leading to a multitude of energetic levels. The total spectral intensity is then distributed among many lines too weak to be recorded.

Let us consider only some of the examples of actual problems, where ato-

mized gases and small radicals play a crucial role and special ESR techniques can deliver valuable data about reaction mechanism and kinetic parameters: gain of energy through oxidation of hydrogen and hydrocarbons, controlled burning in engines and jet motors, civil and industrial use of the flame and study of flame retardant effects, photochemistry and influences of environmental processes, ozone hole and acid rain formation, surface polymerization and mass loss of polymer coatings of flying objects in space (etching), material corrosion near strong energy sources of broadcast emitters, physics of hot and cold plasma and laser effects, initiation of skin and lung cancer, air and medicament sterilization, tumour destruction, spontaneous synthesis of recombinant products from atomized plasma components (*e.g.* H_2O_2 , NH_3 , $\text{NH}=\text{NH}$), selective interaction of metals (Fe, Pt, Pd, Ti) with $\text{H}\cdot$, $\text{D}\cdot$, $\cdot\text{O}\cdot$, $\cdot\dot{\text{N}}\cdot$.

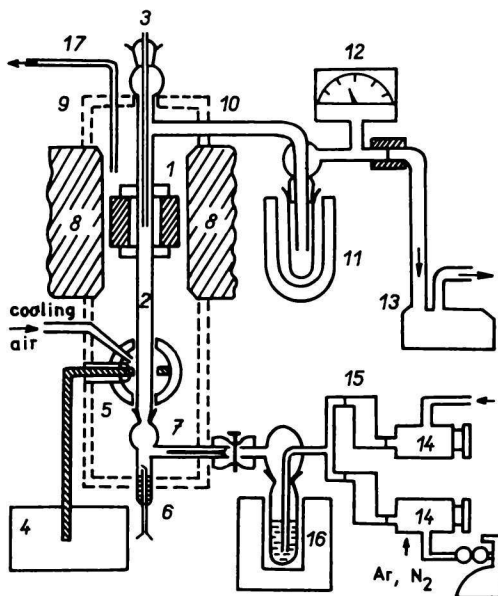
Experimental

Apparatus

In contrast with the horizontal arrangement of the gas-flow experiments in the classical work of *Westenberg* and *de Haas* [7] the detection of species with odd electron in our gas-flow system was performed in a quartz sample tube passing vertically through the ESR cavity (Fig. 1). It enables to set a glass capillary jet coaxially from the top into the sample tube and to lead gases or vapours from the opposite direction against the

Fig. 1. Experimental arrangement for studying the ESR signals of paramagnetic species in the cold plasma generated by the microwave discharge at $\nu = 2450$ MHz, from different gases at lowered pressure.

1. ESR cavity; 2. quartz sample tube; 3. capillary jet (or thermoelement) for cross-flow experiments; 4. source of 2450 MHz microwave radiation; 5. air-cooled electrodes; 6. Pt spark-starter for plasma ignition; 7. capillary inlet of gases; 8. magnet poles; 9. closing polystyrene block with exhaustion; 10. connection to the vacuum line; 11. cooled trap; 12. vacuum meter; 13. vacuum pump; 14. needle valves for gas inlet; 15. gas flowmeter; 16. thermostat for evaporated or with gases bubbled liquids.



incoming radicals and to study reactions between para- and diamagnetic colliding species. Also a thermoelement can be inserted for measuring temperature effects resulting from radical recombination. The other side of the sample tube is closed with a Pt-spark starter to ignite the microwave plasma. With the aid of a side-arm fitted with a quartz capillary, the studied gases or vapours are dosed into the sample tube under control and then they are atomized passing the zone of the microwave cavity. The two electrodes cooled by compressed air in contact with the outside of the quartz sample tube (inside diameter 8 mm) are supplied with microwave radiation ($\nu = 2450$ MHz) with the aid of a 1.5 m long shielded coaxial cable. The microwave power generator was of the type Microtron 200 (Mark III, EMS-Wantage, England) with variable power output 0 to 200 W. The microwave cavity of type 214 L (diameter 13 mm) was prevalingly situated in a distance of 22 cm from the centre of the rectangular ESR cavity operating in the TE_{102} mode.

The gas flows tempered to 23 °C were controlled by calibrated gas-flowmeters and regulated with needle valves. Vapours of H_2O , D_2O , NH_3 , H_2O_2 , CCl_4 , $CHCl_3$, CH_3OH were led to the sample tube by bubbling argon through the relevant liquid stored in a tempered glass vessel.

The absolute pressure in the flow tube was measured with a McLeod gauge and its relative changes were indicated with an electric vacuum manometer situated among the quartz sample tube, the cooled trap and the mechanical pump of $30 \text{ dm}^3 \text{ s}^{-1}$ power.

A Varian E-3 ESR spectrometer was adapted operating in X-band with a 100 kHz field modulation. The cavity with the quartz tube was resonant at the frequency of 9345 MHz.

For relative control of the resonant line intensities the peak height (expressed in arbitrary units, *e.g.* mm) of the resonance at $g = 2.0028$, attributed to the paramagnetic impurities in the quartz tube, as an inner standard, was used. The spin concentration was determined by comparison of the inner standard with the Varian weak (1×10^{13} spin/ 0.3 cm^3) and strong (3×10^{15} spin/ 0.3 cm^3) pitch. The effective volume of gases contributing to the ESR signals in the measured part of the sample tube situated in the ESR cavity (*ca.* 2 cm) was exactly 1 cm^3 after correction on the cosine sensitivity decrease with the distance from the centre of the cavity.

Temperature of the plasma and cyclotron resonance

The temperature measured inside the sample tube in the centre of the cavity with a thermoelement situated 22 cm from the electrodes is a function of the applied microwave power and the actual pressure (Fig. 2).

During routine measurements in the range of 66 up to 200 Pa and at the power P_{mw} between 10 to 40 W, the temperature increase near the top of the cavity is small $\Delta T = 0.3$ —0.8 K. In the central colour-emitting zone, where the flowing molecular gases are atomized by colliding with rapidly moving “hot” electrons, the temperature is the highest one according to the applied microwave power. But in spite of it the surface temperature of the quartz sample tube at $P_{mw} = 20$ W is not higher than 267 K. The electrodes are kept at constant temperature with the aid of streaming compressed air. With increasing power

not only the temperature is increasing, but also the most intense light emitting colour zone (2 cm high at 20 W) is more and more prolonged. At high power and mainly when the distance between the microwave inlet and the ESR cavity centre is decreasing, an increasing number of free electrons in the prolonged hot plasma can reach the inside of the cavity causing a broad resonance absorption overlapping the narrow lines of the studied ESR spectra (Fig. 3). This effect can dominate, when for generation of the paramagnetic species in the gas phase an electric discharge tube with inner electrodes is used, and is explained as the cyclotron resonance of the free electrons [12].

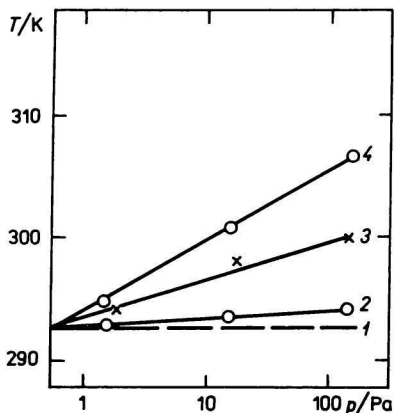


Fig. 2. Increase of plasma temperature with the increase of pressure, when different power of microwave transmitter was applied: 1. 10 W; 2. 25 W; 3. 60 W; 4. 120 W. Constant distance of 22 cm between the microwave radiation cavity and the centre of the ESR cavity.

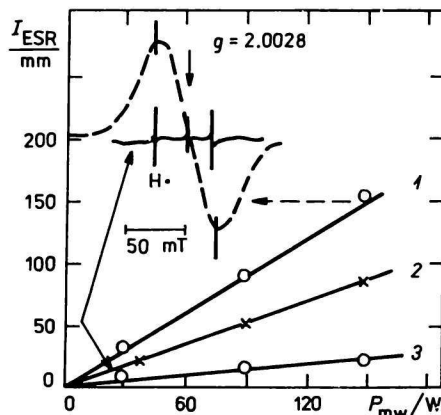


Fig. 3. Dependence of the ESR signal intensity of the cyclotron resonance on the microwave power at different distances of the microwave radiation cavity from the centre of the ESR cavity: 1. 12 cm; 2. 17 cm; 3. 22 cm; and at pressure of 66 Pa.

Spin trapping from gas phase

For indirect detection of paramagnetic species by their trapping from flowing gases, the spin trapper 5,5-dimethyl-1-pyrroline *N*-oxide (DMPO; Sigma, St. Louis, U.S.A.) was used in the form of a layer coating a glass target, situated in the sample tube at different distances from the centre of the cavity. A layer evaporated from a benzene or ethanol solution of DMPO on the inner walls of the cold trap can serve for spin trapping from the condensed medium at decreased temperature (liquid N₂ or solid CO₂). After finishing the time of exposure to radical attack, the spin-adducts are removed from the solid glass support by dissolving in benzene or water. The ESR signals of the dissolved spin-adducts were measured in cylindrical or flat cells with a Bruker SRC-200 ESR

spectrometer. This elaborated technique can be applied for detection of differences in the radical composition of the cold plasma, when the homogeneous magnetic field of the spectrometer is switched on ($B = 300\text{--}500\text{ mT}$) or turned off.

Frozen radicals from cold microwave plasma on internal cryostat in the ESR cavity

For detecting of high reactive free radicals ($\text{HO}\cdot$, $\text{HOO}\cdot$) in the cold microwave plasma at low steady-state concentration below the threshold sensitivity level of the ESR spectrometer a quartz micro-cryostat was coaxially situated in the sample tube passing the T_{102} mode rectangular cavity. Through the central inner capillary gaseous N_2 was continuously pressed being cooled by flowing through a liquid nitrogen reservoir (-194.5°C). The frozen radicals from the microwave plasma accumulate on the outer surface of the cryostat cooled to *ca.* -190°C .

Results and discussion

Hydrogen and deuterium atoms

When molecular hydrogen is flowing through the sample tube, passing the microwave discharge zone, the observed ESR signal is composed of two narrow lines with a splitting constant $a = 50.5\text{ mT}$, characteristic of atomic hydrogen (Fig. 4). The free electron on the s -orbital ($S = 1/2$) is in strong 100 % contact interaction with the proton of the nucleus, possessing a nuclear magnetic moment $I = 1/2$ and the experimental value of the splitting constant is in perfect correlation with the theoretical one according to the Fermi equation [13]. Similarly the observed shift of the centre of the ESR signal symmetry from the position of the g -value of the free electron $g = 2.0023$, $\Delta B = B_0 - B_{\text{eff}} = 2\text{ mT}$,

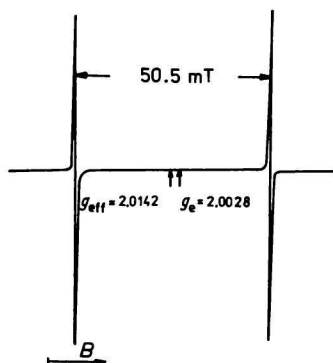


Fig. 4. ESR signal of atomic hydrogen produced by microwave discharge of molecular hydrogen at 66 Pa.

is in very good correlation with the effective values $g_{\text{eff}} = 2.0142$ calculated on the basis of the corresponding spin Hamiltonian. These values, measured in cold plasma zone at 296 K, are exactly the same as we have experimentally proved in the hot zone of hydrogen/oxygen flame near 773 K [14].

The concentration of $\text{H}\cdot$ increases with the applied microwave power (5—75 W) at constant vacuum and reaches its maximum in the vacuum range of 13.3 to 133 Pa with stepwise elevated pressure (Fig. 5) at constant microwave power.

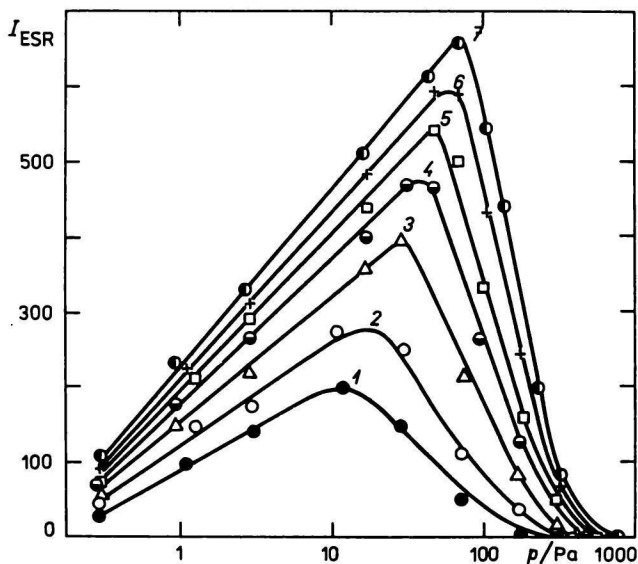
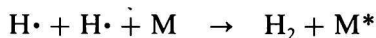


Fig. 5. Dependence of the ESR signal intensity of atomic hydrogen in arbitrary units upon the vacuum, when H_2 is passing the microwave zone at the increased power of microwave transmitter: 1. 5 W; 2. 10 W; 3. 15 W; 4. 30 W; 5. 40 W; 6. 50 W; 7. 75 W.

The decrease of the concentration of $\text{H}\cdot$ passing the maximum down to zero at constant power is explained by the increased probability of the recombination rate at elevated pressure and by the transfer of the evolved recombination heat to the wall (M) of the sample tube with increased number of forming molecules of hydrogen



In the same experimental conditions a comparatively higher concentration of $\text{H}\cdot$ is produced from water evaporating in the vacuum in a slow argon stream passing the microwave zone, than from dried hydrogen molecules (Fig. 6). The

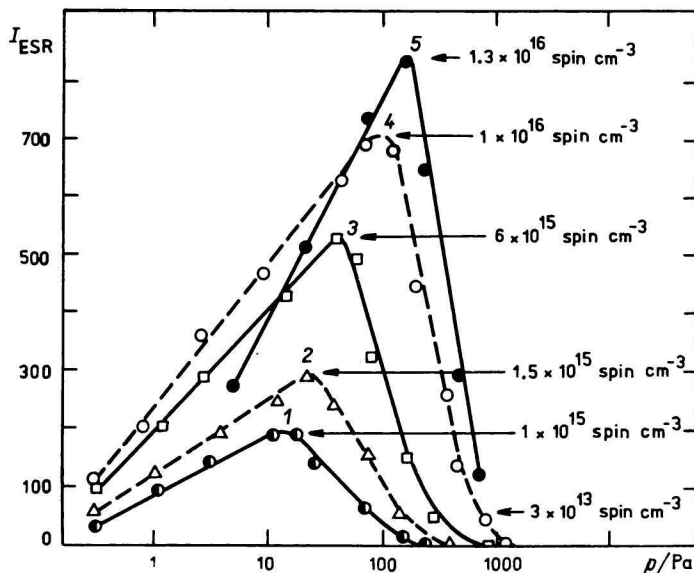


Fig. 6. Dependence of the ESR signal intensity on the pressure for atomic hydrogen (1–4) or atomic deuterium (5) generated by 5 W (1, 2) and 50 W (3–5) power of the microwave discharge, when H_2 , H_2O or D_2O vapours in argon stream are atomized. The maximum number of spins in 1 cm^3 is indicated.

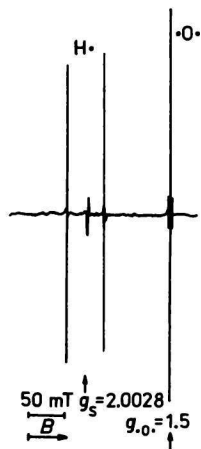


Fig. 7. ESR signal of atomic hydrogen and oxygen of decomposed water molecules in argon stream generated at pressure of 120 Pa and $P_{\text{mw}} = 20 \text{ W}$.

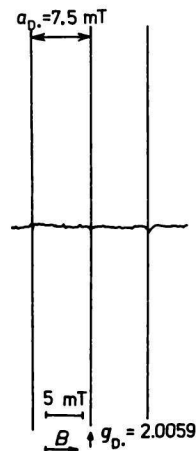


Fig. 8. ESR signal of atomic deuterium produced by microwave radiation ($P_{\text{mw}} = 20 \text{ W}$) from D_2O in argon stream at pressure of 530 Pa.

ESR signal is composed of the hydrogen atom doublet at $g = 2.0142$ and of the nonresolved line of atomic oxygen at $g = 1.5$ (Fig. 7).

Heavy water D_2O in the argon stream is decomposed by the microwave radiation to deuterium atoms $D\cdot$ giving the characteristic three equi-intense lines ($I = 1$) at $g = 2.0059$ (Fig. 8) [15, 16]. The decrease of the g -value in comparison with hydrogen atoms as well as of the splitting constant from 50.5 mT to 7.5 mT results from the negative magnetic moment μ of the neutron, reducing the magnetic effect of the proton in the deuterium nucleus. According to the difference between the splitting constants of $H\cdot$ and $D\cdot$ in the sense of the Fermi equation [13] $\mu = -1.911 \times 5.058 \times 10^{-27} \text{ JT}^{-1}$ calculated from ESR experimental data is in excellent agreement with $\mu = -1.91315 \times 5.058 \times 10^{-27} \text{ JT}^{-1}$ determined by NMR. The presence of DHO in equilibrium with D_2O is indicated on the basis of the doublet $H\cdot$ near the triplet $D\cdot$ lines (Fig. 9).

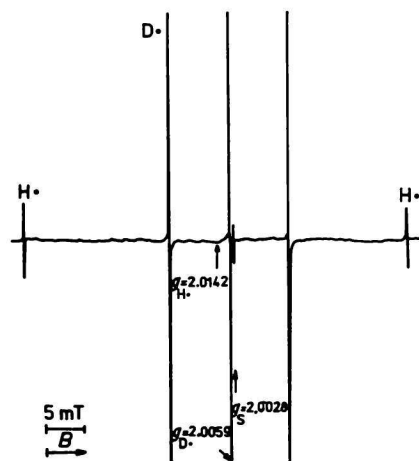


Fig. 9. ESR signal of atomic deuterium and atomic hydrogen in the cold microwave plasma generated from D_2O in the presence of H_2O traces at pressure of 160 Pa.

D_2O containing H_2O or H_2O_2 bubbled with a slow argon stream and led through the microwave zone, shows a complete atomization of all molecules, demonstrated in ESR with the signals of $H\cdot$, $D\cdot$, and $\cdot O\cdot$ (Fig. 10).

So far the atomization proceeds with exclusion of water traces, the reached maximum of spins in 1 cm^3 volume of the sample tube in the cavity is *ca.* 6×10^{15} , which represents *ca.* 30 % presence of $H\cdot$ in the gas phase (at 50 W power), but 70 %, when the decomposition proceeds from water ($1.5 \times 10^{16} \text{ spin cm}^{-3}$). From D_2O the spin concentration of $D\cdot$ can reach, at the same conditions, *ca.* $2 \times 10^{16} \text{ spin cm}^{-3}$. It indicates lowering of the recombination rate of $D\cdot$ in comparison with $H\cdot$ atoms.

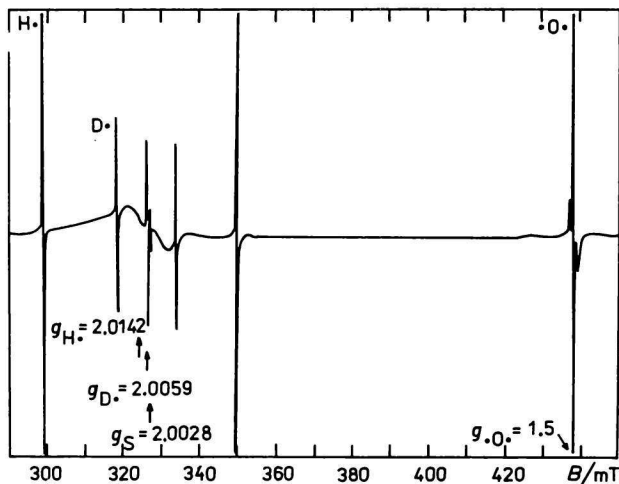


Fig. 10. ESR signal of atomized hydrogen, deuterium and oxygen in the cold plasma formed from the mixture of D_2O , H_2O , and H_2O_2 in the mole ratio of 2:3:1 in argon stream at pressure of 270 Pa. The microwave frequency of the clystron was 9.415 GHz.

Atomic oxygen and nitrogen

In the previously described ESR spectra of atomized H_2O and D_2O vapours the narrow line at $g = 1.5$, belonging to atomic oxygen with two unpaired electrons, was not resolved. But at low pressure near or below 1.3 Pa, when molecular oxygen is flowing through the sample tube after passing the zone of microwave radiation, the ESR spectrum is split to different number of lines according to the actually applied power of the ESR clystron ($\nu = 9415$ MHz) in the range of 0.8 up to 240 mW (Fig. 11). For high resolution of all lines a modulation of 0.05 mT and a very slow registration time is required.

When no saturation takes place (at 0.8 mW), the $\bullet O\bullet$ spectrum consists of two sets of lines. The four more intense lines in the centre of the spectra result from the five M_J levels of ground state 3P_2 in consequence of the strong spin-orbital coupling between the two unpaired electrons ($S = 1$) and the p -orbital ($L = 1$, $J = L + S = 2$, number of levels $2J + 1 = 5$). The two weaker lines on both the sides belong to the three M_J levels of the $^3P_1^*$ excited state ($L = 0$, $S = 1$) lying 158.5 cm^{-1} above the ground state [1, 17]. With stepwise increase of the clystron power the original four lines of 3P_2 are superimposed with three new additive lines. After reaching a maximum the intensity of the four lines begins to be saturated and the three-line signal increases to its maximum (Fig. 12). With further saturation the decrease of the three-line signal is followed with the increase of two lines and at $P_{mw} = 240$ mW in the centre of the signal dominates one line. At power over 100 mW the two lines of the excited state $^3P_1^*$ are fully saturated and unobservable.

The schematic diagram (Fig. 13), taking into account the splitting of energet-

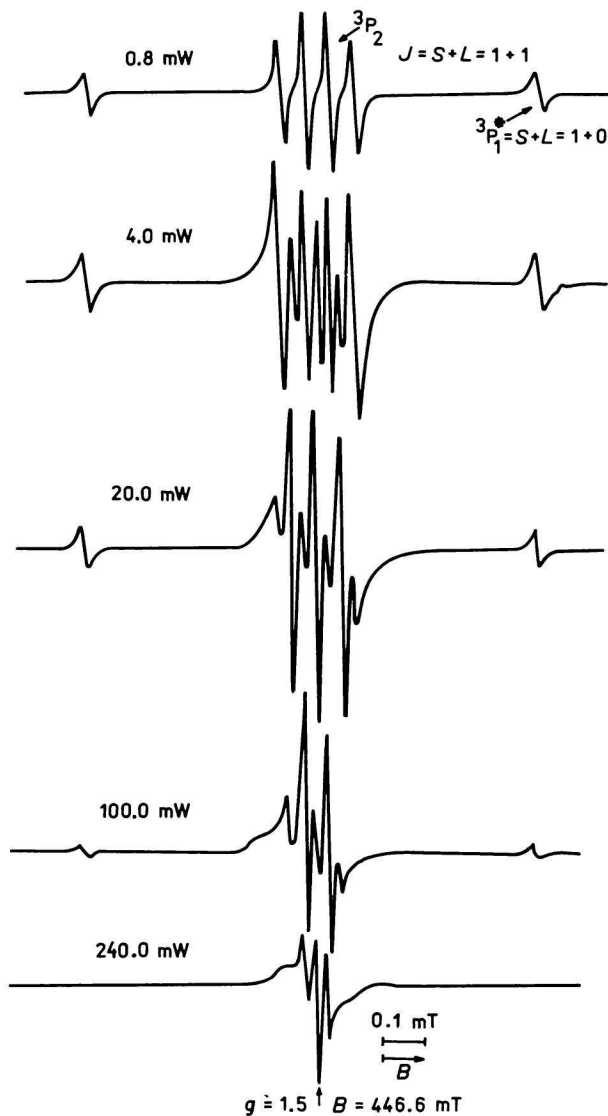


Fig. 11. Changes of the atomic oxygen ESR signal with increasing clystron power (0.8 → 240 mW) at constant power of the microwave discharge (15 W at 1.3 Pa). The resonance frequency of the clystron was 9.415 GHz.

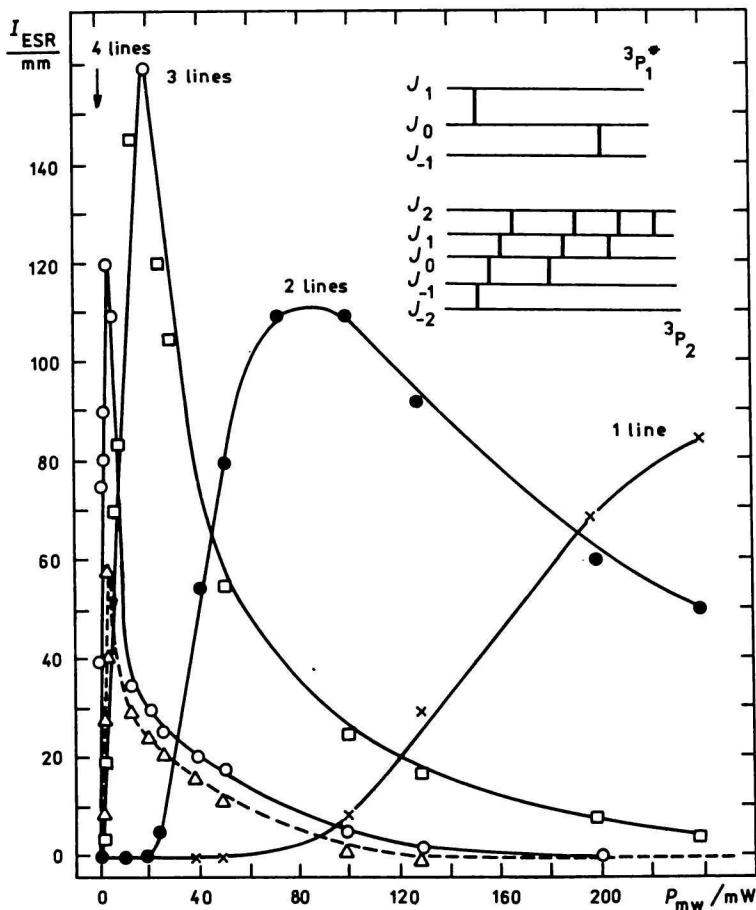


Fig. 12. Dependence of the intensity of ESR signals belonging to different sets of lines at stepwise saturation on increasing power of the clystron. The full lines belong to atomic oxygen in the ground state 3P_2 and the dotted line to the excited state $^3P_1^*$.

ic levels, already in the zero magnetic field ($\Delta E_{3p_2}, \Delta E_{3p_1}$), gives explanation of the described saturation phenomenon. The theory is based on gas phase study of oxygen atoms reported by *McDonald* [6] and on observations of *Rawson* and *Beringer* [3]. The latter authors passed an efficient oxygen-gas stream from an electric discharge through a quartz tube into the ESR cavity decreasing gradually the microwave attenuation and elaborated a more-quantum transition model. Within the 3P_2 ground state it is possible to observe at low power input the four 1-quantum transitions, after saturation of the lower level $M_J = -1$ three 2-quantum transitions, after saturation of the level $M_J = 0$ two 3-quantum

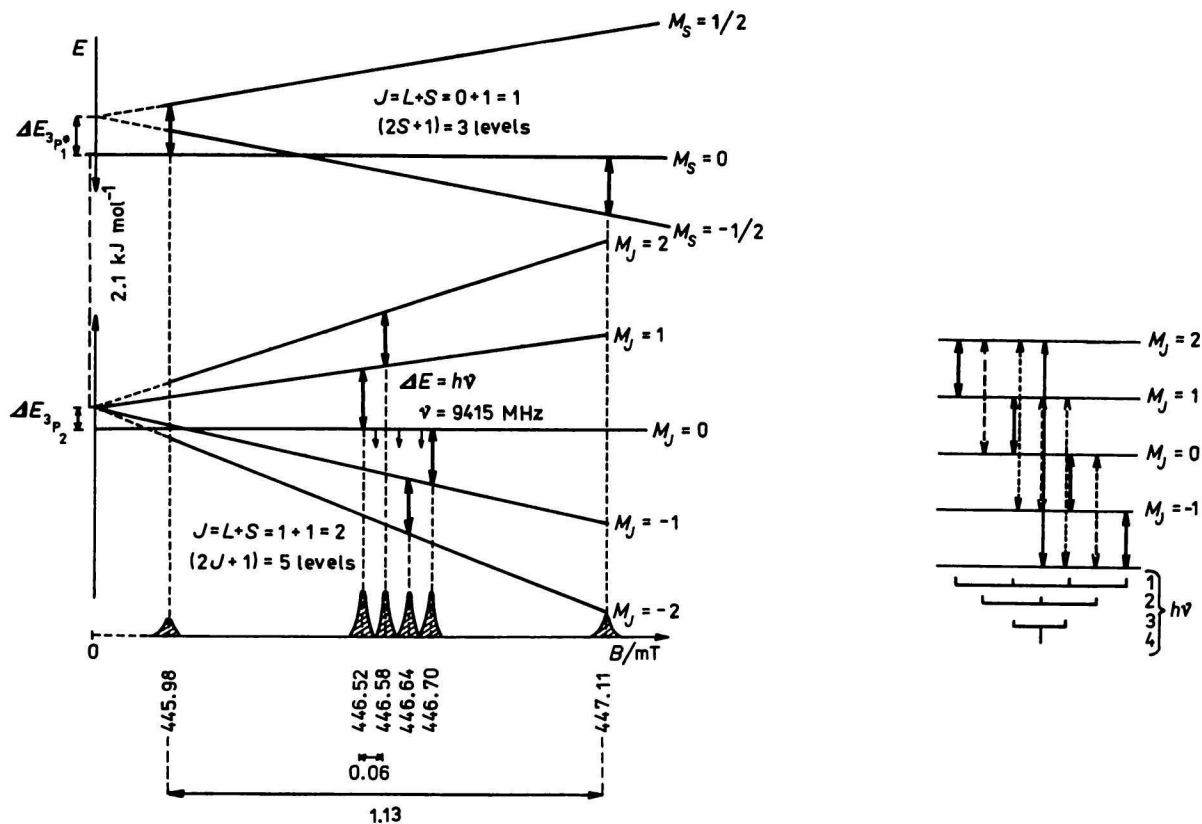


Fig. 13. Energetic levels of atomic oxygen in the ground state 3P_2 and in the excited state $^3P_1^*$ as a function of the applied magnetic field. Scheme of stepwise saturation of energetic terms and many-photon transfer. The difference in the energy between the two levels calculated for 1 mol excitation is 2.09 kJ mol $^{-1}$.

transitions, and after saturation of $M_j = 1$ level with the highest microwave radiation input the one 4-quantum transition.

In all of our following experiments between atomic oxygen and different diamagnetic gases only the nonresolved ESR signal of $\cdot\text{O}\cdot$ was measured (the 1-quantum transition employing 10 mW power of the clystron). The high precision of the measurements is documented from the comparison of the calculated value of $g_{\cdot\text{O}\cdot}$ determined from the Landee expression

$$g_{\cdot\text{O}\cdot} = 1 + \frac{J(J+1) + S(S+1) - L(L+1)}{2J(J+1)} = 1.5$$

with experimentally obtained $g_{\text{exp}} = 1.493$.

The concentration of atomic oxygen is a function of the applied microwave power and attains a maximum near 133 Pa with increasing pressure (Fig. 14). At similar experimental conditions for atomic hydrogen the maximum is reached at 40 Pa and for atomic nitrogen at 80 Pa. The number of spins in 1 cm^3 at the maximum is 5×10^{15} for atomic nitrogen, 6×10^{15} for atomic hydrogen and 8×10^{15} for atomic oxygen, which represents 30 to 50 vol. % of atomized species

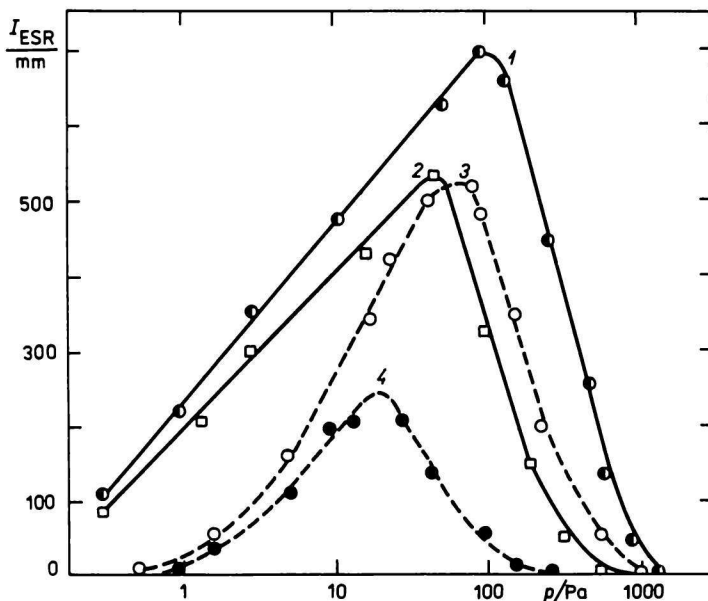


Fig. 14. Dependence of the intensity of ESR signal of atomic oxygen (1), hydrogen (2), and nitrogen (3, 4) on the pressure at 40 W (1–3) and 15 W (4) microwave power ($\nu_{\text{mw}} = 2450 \text{ MHz}$) and applied 25 mW power of the ESR clystron ($\nu_{\text{c}} = 9415 \text{ MHz}$).

in the cold zone of the microwave plasma. When we compare these values with the relevant bond energies (in kJ mol^{-1}) of N_2 (946), O_2 (491) and H_2 (423), and with the amount of dissolved molecules produced thermally at 4000°C (in vol. %): N_2 (2.9), O_2 (61), H_2 (82), the effective kinetic energy of electrons of the microwave discharge decomposing the molecules, must be equivalent to a temperature of order of 5000°C , when 26.2 % of thermally dissociated nitrogen is observed. The input energy is concentrated into the relatively small volume of the sample tube near the direct contacts with the electrodes. In this "hot" zone the diatomic molecules consume the greatest part of the energy for dissociation and not for excitation of the rotation and of the vibration energetic levels. In the nucleus of the electromagnetic discharge the number of free electrons increases with pressure and its surface density can reach 8×10^{15} electrons/ cm^2 (when a 8 mm diameter sample tube is used). In general it is accepted [18] that the atomization results from the collisions of the molecules with electrons possessing enough energy for excitation, dissociation and ionization. In the range of 10–150 W power a high degree of dissociation and ionization is reached without remarkable heating on the streaming gases and so the greatest part of atoms pass the ESR cavity remaining in their ground state. Only in the case of atomic $\cdot\text{O}\cdot$ approximately 12 % are excited from the $^3\text{P}_2$ ground state to the $^1\text{P}_2$ state.

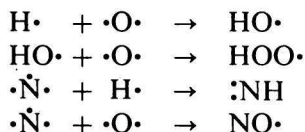
The only state concerning the atomic nitrogen is the $^4\text{S}_{3/2}$ ground state with three unpaired electrons ($S = 3/2$, $L = 0$, $J = 3/2$) and with four M_J levels. The ESR signal of the atomic nitrogen is composed of three equally intense lines separated with the splitting constant of 0.375 mT and with $g = 2.0040$ (Fig. 15). Since N^{14} has a nuclear spin of $I = 1$, each of the four M_J levels is split into three sublevels corresponding to $M_I = 0, \pm 1$ in the strong field of the applied X-band ESR. According to calculations of *Adrian* [19] there is supposed a configuration interaction of the $2s^1 2p^4$ state with the $2s^2 2p^3$ ground state responsible for the isotropic hyperfine splitting $a_{\text{N}} = 0.375$ mT, leading to three triply degenerated lines of equal intensities [7].

Atomization of volatilized molecules containing carbon atoms

Evaporized methyl alcohol, when decomposed in the microwave plasma to its atoms, reveals beside the hydrogen atom doublet and the nonresolved singlet line of atomic oxygen, also an asymmetric narrow line (0.3 mT) at $g \doteq 2.000$, split to a doublet ($a = 0.08$ mT). This signal remains stable at ambient temperature also after turning off the microwave plasma for some weeks. The signal corresponds to the black deposit (partially soluble in benzene) on the inner surface of the quartz sample tube. This signal can be ascribed to soliton defects in the polyacetylene deposit as a product of $\text{CH}\cdot$ radical recombination.

Radical reactions in the gas phase

When H_2O or D_2O , NH_3 , H_2O_2 are bubbled with nitrogen or mixtures of different gases (H_2 , O_2 , N_2 , NO) are introduced into the microwave discharge zone, the observed ESR spectra are always composed only of lines of the individual atomized gases $\text{H}\cdot$, $\text{D}\cdot$, $\cdot\text{O}\cdot$, $\cdot\dot{\text{N}}\cdot$ (Fig. 16; 1 and 2), and no signals of secondarily formed radicals



are observed.

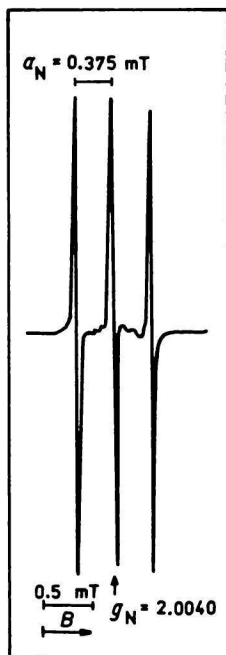


Fig. 15. ESR signal of atomic nitrogen at 260 Pa.

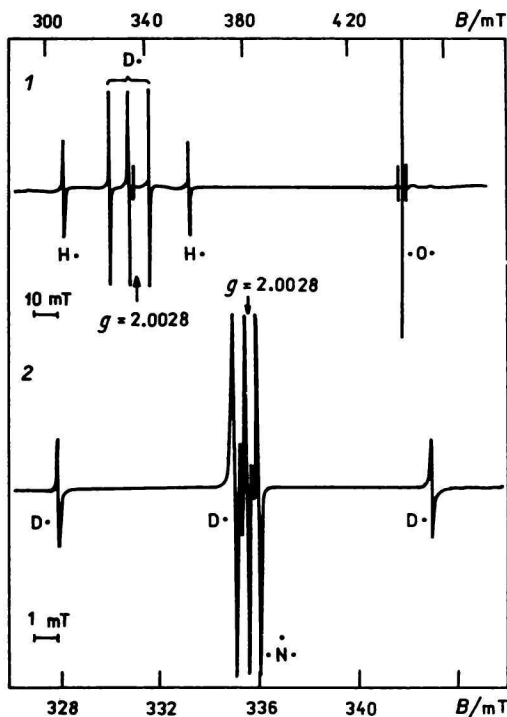


Fig. 16. ESR signal of atomic hydrogen, deuterium, and oxygen, when D_2O in argon stream (1) and in nitrogen stream (2) is decomposed with microwave radiation.

The simultaneous presence of four different atomized gases $\cdot\text{O}\cdot$, $\cdot\dot{\text{N}}\cdot$, $\text{D}\cdot$, and $\text{H}\cdot$ with high concentration in the cold plasma can be proved, when vapours of D_2O (containing H_2O and DHO) are carried with the streaming nitrogen through the microwave zone before passing the ESR cavity. The central line of the three-line signal of the atomized deuterium ($a_{\text{D}} = 7.6 \text{ mT}$) is superimposed on the intense three-line signal of atomized nitrogen ($a_{\text{N}} = 0.35 \text{ mT}$) (Fig. 16; 2). This signal was absent, when instead of nitrogen heavy water was bubbled with argon, but still the intensity relations between the $\text{D}\cdot$, $\text{H}\cdot$, and $\cdot\text{O}\cdot$ lines remain unchanged (Fig. 16; 1). Effective radical recombination on the walls of the sample tube starts after release of the plasma from the homogeneous magnetic field of the ESR spectrometer.

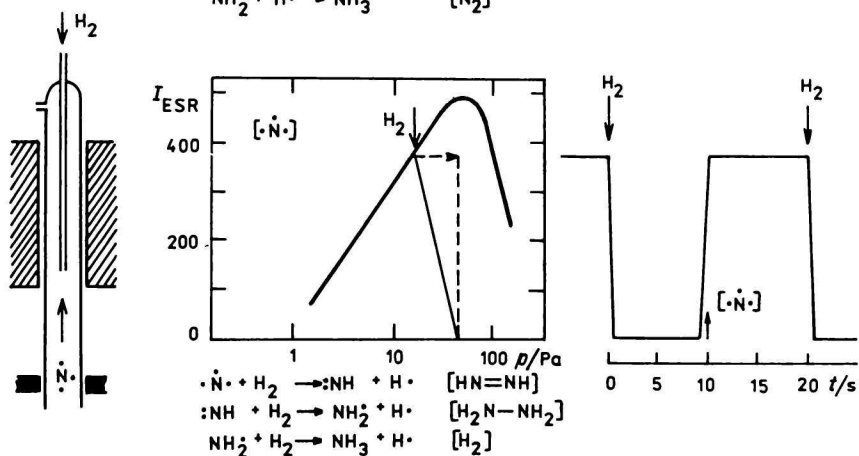
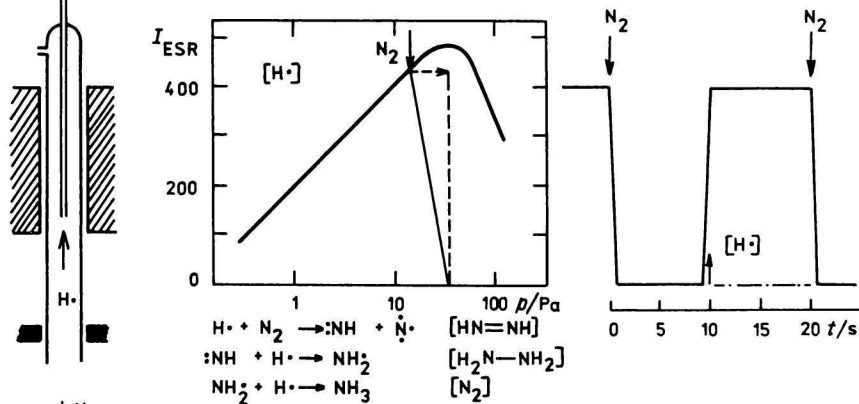
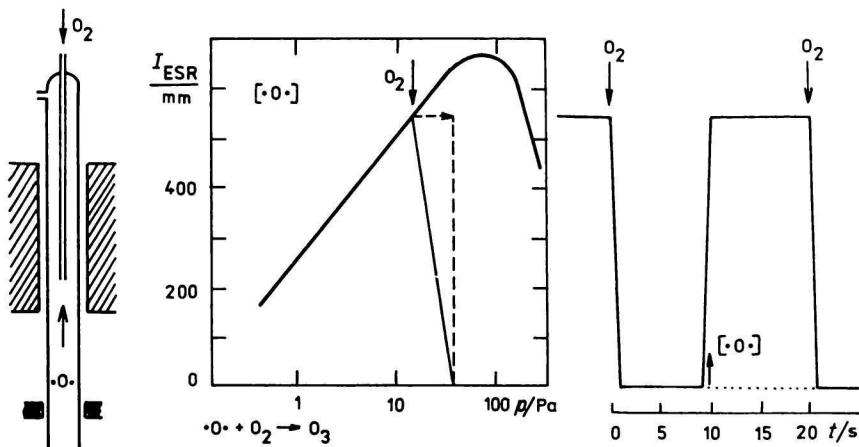
On the other hand, reactions in the homogeneous magnetic field between the partially oriented paramagnetic molecules of gases and the nonoriented diamagnetic molecules proceed with high speed already at ambient temperature. Atomized gases coming into the cavity from the bottom collide with molecules flowing from the top through a quartz capillary jet situated below the centre of the cavity. To avoid the decrease of the number of paramagnetic species only in the consequence of their recombination on the wall of the sample tube at higher pressure, the total pressure during the collision of the both reactants was kept constant under 66 Pa. In this way the cross-flow reactions were controlled not to run over the maximum of experimental curves $I_{\text{ESR}}-p$.

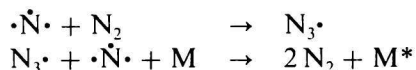
The schematic arrangement of the cross-flow technique, the relevant concentration relations of $\cdot\text{O}\cdot$, $\text{H}\cdot$, and $\cdot\dot{\text{N}}\cdot$ with pressure and the time dependences of the ESR signal intensities (I_{ESR}), when traces of molecules were led in the cavity, are seen in Fig. 17.

In a time period of 1 to 2 s after opening the needle valve for O_2 , the signal of the atomic oxygen disappears, but can be instantly renewed, when the O_2 coming from the opposite direction is stopped. No signals of the molecular oxygen (rotation interaction lines) can be seen, which indicates the transformation of atomic oxygen to ozone



Similar experiments, where $\text{H}\cdot$ reacts with colliding N_2 or when $\cdot\dot{\text{N}}\cdot$ reacts with H_2 in cross-flow arrangement, prove the formation of NH_3 and further products of radical recombination $\text{NH}=\text{NH}$, $\text{H}_2\text{N}-\text{NH}_2$ detected in the cooled trapped condensate (78 K). When $\cdot\dot{\text{N}}\cdot$ reacts in cross-flow experiment with N_2 , the time dependence of the three-line ESR signal proceeds analogically, traces of molecular nitrogen eliminate in one second the signal of atomic nitrogen, which is immediately renewed, when the incoming N_2 is stopped. The transiently formed $\text{N}_3\cdot$ recombines with atomic nitrogen, when contacting the wall (M):





But during the cross-flow experiments, when O_2 collides with $\text{H}\cdot$ or $\text{D}\cdot$ atoms, the expected ESR signal of $\text{HO}\cdot$ or $\text{DO}\cdot$ radicals was not detected.

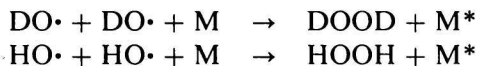
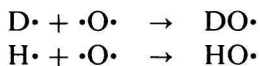
A rapid chlorine atom abstraction proceeds, when tetrachloromethane reacts with colliding $\text{H}\cdot$ or $\cdot\text{O}\cdot$ components of the plasma. The ESR lines of $\text{H}\cdot$ or $\cdot\text{O}\cdot$ disappear instantly, when traces of CCl_4 flowing from the opposite direction, collide with the atomized gases. Atomic chlorine produced under the microwave radiation reacts preferably with atomic oxygen, when other atomic gases as $\text{H}\cdot$, $\text{D}\cdot$, or $\cdot\dot{\text{N}}\cdot$ are present, forming $\text{ClO}\cdot$ and $\text{ClO}_2\cdot$ and finally the products of the recombination ClOCl and ClOOC .

Reaction of the molecular oxygen with atomized molecules of water

Under decreased pressure of 50 Pa, when dried O_2 flows through the sample tube, the observed spectrum is composed of many narrow lines resulting from the resonance between magnetic Zeeman levels mixing with individual rotation terms of the molecular oxygen (Fig. 18; 1) [9]. The most intense lines are signed as A, B, B_1 , B_2 , C, D, E, in direction of the increasing induction of the magnetic field (500 \rightarrow 700 mT).

Vapours of D_2O (DHO) carried with the streaming argon through the microwave radiation zone are completely atomized and the ESR signal is composed of the nonresolved singlet line of $\cdot\text{O}\cdot$, triplet of $\text{D}\cdot$ and doublet of $\text{H}\cdot$ (Fig. 18; 2). When against the flow of O_2 at 50 Pa the atomized components of the plasma are streaming from the opposite direction into the cavity, the multi-line ESR signal belonging to molecular oxygen, as well as the unresolved signal of $\cdot\text{O}\cdot$ immediately decreases (Fig. 18; 3) in consequence of the reaction leading to diamagnetic ozone $\cdot\text{O}\cdot + \text{O}_2 \rightarrow \text{O}_3$. After increasing the pressure of oxygen to 300 Pa the O_2 (rot) spectrum is partially renewed and the lines of atomized deuterium and hydrogen disappear (Fig. 18; 4) in consequence of recombination to peroxides

Fig. 17. Schematic arrangement of the cross-flow technique, in which the atomic oxygen collides with O_2 , atomic hydrogen with N_2 , and atomic nitrogen with H_2 . Dependence of the ESR signal intensities on the pressure and indication of the signal disappearance after inlet of O_2 , N_2 or H_2 into the sample tube. Time dependence of the signal intensity of $\cdot\text{O}\cdot$, $\text{H}\cdot$, and $\cdot\dot{\text{N}}\cdot$ in the course of interrupted inlet and stop-flow of O_2 , N_2 or H_2 gases alternatively in *ca.* 10 s intervals.



Nevertheless the direct proof of the transiently formed HO· radicals on the basis of their known ESR signal in gas phase ($g \approx 1.14$, $B_0 \approx 580$ mT, $\nu = 9.34$ GHz) during the reaction of atomic oxygen with H₂O, or DO·, when ·O· reacts with D₂O, failed. One explanation of this negative result is based on the assumption that the steady-state concentration of the highly reactive HO· radicals lies under

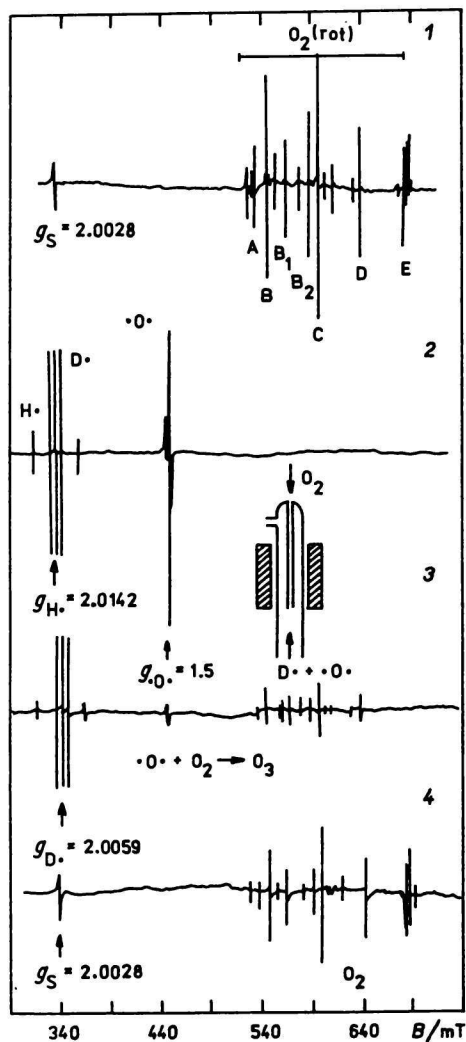


Fig. 18. ESR signal of molecular oxygen at 50 Pa (1), of cold plasma generated by microwave radiation from D₂O vapours in argon stream (2), cross-flow experiment between atomized deuterium, oxygen and molecular oxygen at 50 Pa (3) and at 300 Pa (4).

the threshold sensitivity level of the ESR technique, when secondary reactions constantly decrease the number of the HO• radicals in the plasma, namely when atomic oxygen is present



followed with recombination reactions



The other explanation is based on the fact that the HO• signal cannot be detected with the cavity employed, because its ESR transition is of the electric dipole type [10, 11]. On the other hand, well resolved doublet signal ($I = 1/2$, $a_{\text{H}} = 2 \text{ mT}$) with further three-line splitting ($J = 3/2$, $a_{\text{J}} = 0.2 \text{ mT}$) of HO• radicals was obtained in the post-flame region of a stoichiometric methanol—air flame using a large access cylindrical cavity TE₁₀₂, where both the magnetic and electric dipole transitions are detectable [20].

Indirect detection of HO• and HOO• radicals in plasma reactions

To prove the presence of HO• radicals in the studied gas phase reactions, when hydrogen is abstracted from water in the presence of •O•



an indirect method using DMPO as spin trapper, transforming the reactive HO• radicals to stable nitroso spin-adducts, was elaborated. When •O• atoms of comparatively high concentration collide with H₂O molecules of very low concentration ($[\cdot\text{O}\cdot] > [\text{H}_2\text{O}]$), the ESR signal is composed of the intense line of •O• and of very weak lines of O₂ (rot) and H• (Fig. 19; A, I), which explains the disappearance of the primarily formed HO• radicals in consequence of the following reaction



Increasing the H₂O pressure by increasing the thermostat temperature from 253 K to 293 K, followed with pressure increase from 80 Pa to 213 Pa ($[\cdot\text{O}\cdot] < [\text{H}_2\text{O}]$), in the first 20 s the signal of •O• decreases (originally *ca.* 6×10^{15} spin cm⁻³) as well as the signal of O₂ (rot) and H• (originally *ca.* 6×10^{14} spin cm⁻³) to zero (Fig. 19; B, 2).

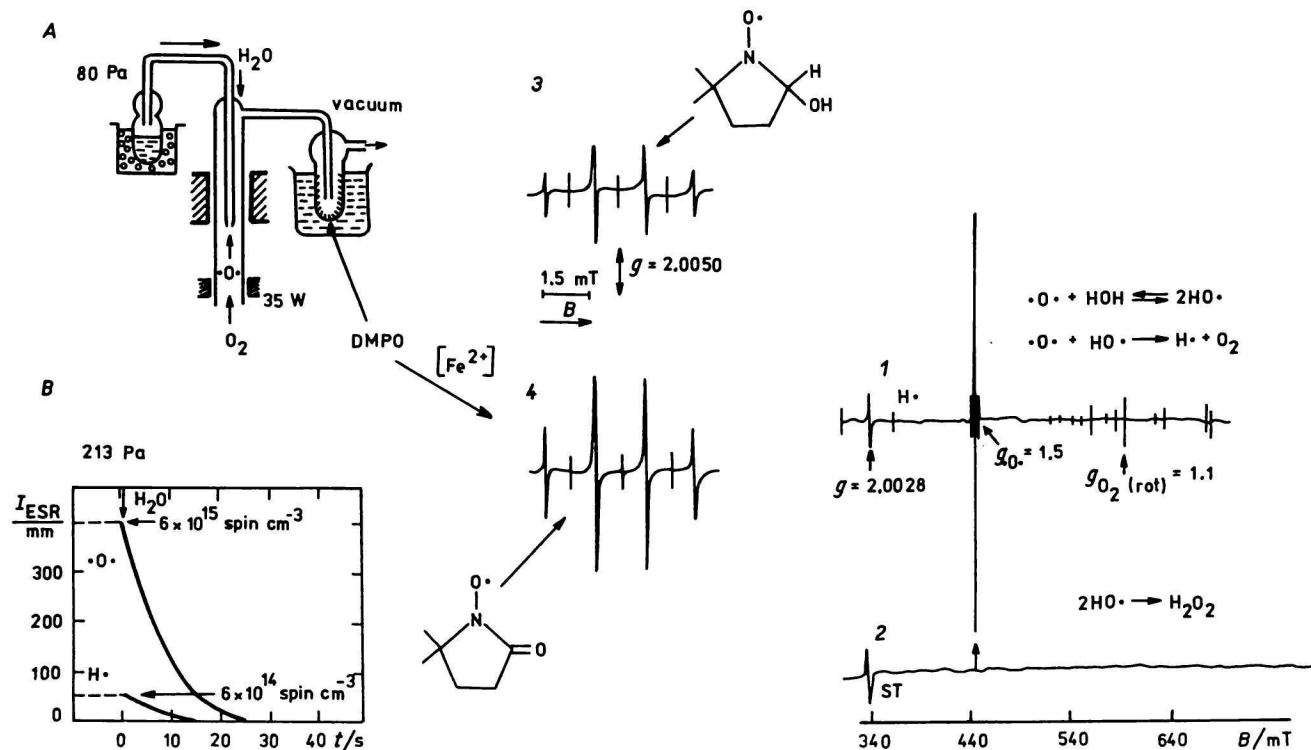
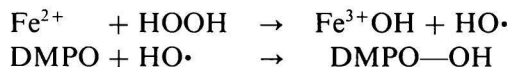


Fig. 19. Experimental arrangement for cross-flow reaction between atomic oxygen and water molecules with simultaneous trapping of free radicals in the cooled condensate with DMPO (A). ESR signal at low partial pressure of water vapours, when the H_2O storage is frozen at 253 K in vacuum ($p = 80 \text{ Pa}$) in high mole surplus of atomic oxygen, $[\text{O}\cdot] > [\text{H}_2\text{O}]$ (1) and at increased concentration of water molecules at 293 K and pressure of 213 Pa, when $[\text{O}\cdot] < [\text{H}_2\text{O}]$ (2). Decrease of line intensities belonging to atomic oxygen and atomic hydrogen with time, when the inlet of H_2O is started (B), ESR of the spin-adduct in the condensate (3) and its change, when crystalline hemin (Fe^{2+}) is admixed (4). ST is signal of the inner standard.

The gases exhausted from the cavity are continuously condensing in the cold trap (78 K) localized between the cavity and the vacuum line.

Before starting the experiment the inner wall of the cold trap is covered with an evaporated layer of the spin-trapper (2 mg DMPO dissolved in 1 cm³ ethanol), after finishing the experiment (40 min, 10 cm³ of condensate) the cold trap is heated to 296 K and 1 cm³ of the liquid condensate is transferred in a flat ESR cell. The four-line ESR signal (1:2:2:1) $g = 2.0050$, is typical for the stable nitroxy spin-adduct of HO• radicals with DMPO ($a_N = 1.5$ mT, $a_H = 1.5$ mT) [21], (Fig. 19; A, 3). A three-line signal characteristic of the final oxidized form of the DMPO adduct ($a_N = 1.35$ mT) is also present. Chelated Fe(II) given to the previous sample is followed with doubling the quartet signal of the HO• nitroxy spin-adduct, while the triplet signal remains unchanged (Fig. 19; B, 4). This fact proves the presence of H₂O₂ in the water condensate as one of the final products of recombination during the reaction of atomic oxygen with H₂O

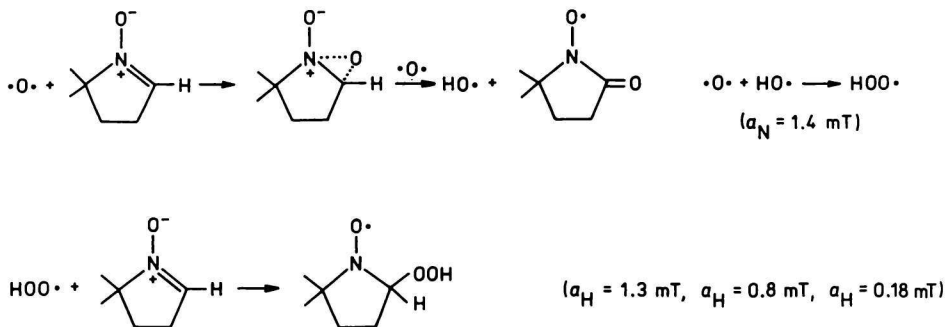


A quartz tube (diameter 4 mm) coated with an evaporated DMPO sheet can be inserted from the top into the sample tube being so in direct contact with the plasma flowing out from the cavity. After finishing the programmed contact time with atomized gases and radicals, the formed spin-adducts are dissolved in 0.5 cm³ benzene from the inserted quartz tube and their ESR signals are analyzed after bubbling the solvent with N₂.

Applying this method, new additional information about all paramagnetic species with low steady-state concentration present in the cold plasma can be obtained. The ESR spectrum of spin-adducts after 20 min contact of plasma with the spin-trapper DMPO (66 Pa, 30 W) is prevailingly composed of different signals of individual spin-adducts. According to spectrosimulation five basic types of signals, belonging to trapped H•, HO•, HOO•, •O•, and R•, were deciphered (Fig. 20). The amount of trapped radicals is higher, when the procedure proceeds at exclusion of the ESR magnetic field for trapped •O• about seven-times, for trapped H• about three-times. This can be explained on the basis of alignment and spin orientation of paramagnetic species in the homogeneous magnetic field lowering the probability of their common recombination, as well as their reaction with the surface layer of the spin-trapper. So the secondary radical reaction can take place, when dried O₂ is atomized, but simultaneously the magnetic field is turned off. The ESR signal composed of two spin-adducts of •O• and HOO• in the mole ratio 1:1 can be explained as follows (Scheme 1).

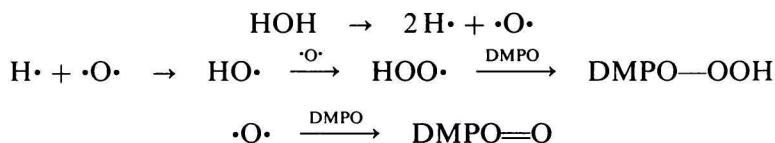
The intensity of the DMPO—OOH signal varies with the presence of water

I			$a_N = 1.45 \text{ mT}$ $2a_H = 2.10 \text{ mT}$
II			$a_N = 1.45 \text{ mT}$ $a_H = 2.00 \text{ mT}$
III			$a_N = 1.50 \text{ mT}$ $a_H = 1.50 \text{ mT}$
IV			$a_N = 1.30 \text{ mT}$ $a_H^\beta = 0.80 \text{ mT}$ $a_H^\gamma = 0.155 \text{ mT}$
V			$a_N = 1.35 \text{ mT}$
Mixed adducts			
$c(I) : c(II) = 3 : 1$			A
$c(I) : c(III) = 2 : 3$			B
$c(I) : c(III) : c(V) = 3 : 4 : 3$			C



Scheme 1

vapours in gases passing through the microwave zone. When carefully dried H_2 is atomized, the nine-line signal ($a_{\text{N}} = 1.45 \text{ mT}$, $2a_{\text{H}} = 2.10 \text{ mT}$) (Fig. 20; *I*) of the DMPO—H spin-adduct dominates, but with increasing humidity the original ESR signal is superimposed on the lines belonging to the spin-adduct of $\text{HOO}\cdot$ (Fig. 20; *IV*). The comparatively highest concentration of trapped $\text{HOO}\cdot$ radicals, 12 % in the additive spectrum, can be obtained, when water molecules carried by argon stream are atomized. The dominating three-line signal (88 %) belongs to the $\cdot\text{O}\cdot$ spin-adduct (Fig. 20; *V*)

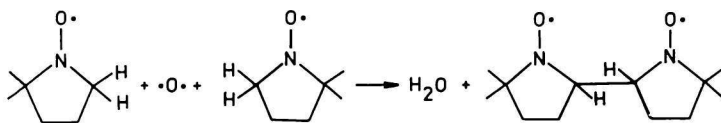


Additionally also signals composed of six lines are admixed to the multicomponent spectrum (Fig. 20; *II*). The splitting constants are typical for spin-adducts of alkyl radicals DMPO—R, probably as products of dimerization



Fig. 20. Simulated ESR signals and the competent splitting constants a of the following DMPO spin-adducts: $\text{H}\cdot$ (*I*), $\text{R}\cdot$ (*II*), $\text{HO}\cdot$ (*III*), $\text{HOO}\cdot$ (*IV*), $\cdot\text{O}\cdot$ (*V*). Superimposed ESR signals of different spin-adducts from the cold microwave plasma formed by decomposing dried H_2 without (*A*) and with (*B*) the simultaneous effect of the homogeneous magnetic field. Presence of 10 % of O_2 in H_2 during atomization under the simultaneous influence of the magnetic field on the cold plasma (*C*).

(Scheme 2) of the primary spin-adducts of DMPO—H in the final phase of surface reactions.

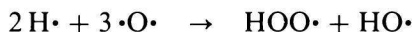


Scheme 2

The composition of accumulated spin-adducts is different, when the spin-trapper DMPO is exposed to $\text{H}\cdot$ downstream from the microwave plasma region under the simultaneous effect of the homogeneous magnetic field or without it. Under influence of the magnetic field the additive ESR signal is composed of 40 % of DMPO—H (*I*) and 60 % of DMPO—R (*II*), (Fig. 20; *B*), in contrast to a relation of 75 % of DMPO—H (*I*) and 25 % of DMPO—R (*II*), when the magnetic field is turned off (Fig. 20; *A*). When oxygen (*e.g.* 10 %) is admixed to the inlet of H_2 , also the contribution of the DMPO=O spin-adduct to the additive ESR signal is seen: 30 % (*I*), 40 % (*II*), 30 % (*V*) (Fig. 20; *C*). It was already mentioned that in spite of the low steady-state concentration of $\text{HO}\cdot$ and $\text{HOO}\cdot$ radicals their presence in cold plasma can be ascertained indirectly in a cross-flow experiment according to the spin-adducts accumulating in the cold trap. When atomized oxygen collides with H_2O , the additive signal of spin-adducts is in relation 50 % DMPO—OH (*III*), 30 % DMPO=O (*V*), 20 % DMPO—OOH (*IV*). This relation between different spin-adducts is changing according to the actual experimental conditions.

In spite of the fact that in the flowing cold microwave plasma the direct evidence of $\text{HO}\cdot$ and $\text{HOO}\cdot$ radicals, using a T_{102} mode rectangular ESR cavity failed and only applying the indirect spin-trapping technique their presence was indicated, this type of cavity can be successfully applied, when the $\text{HO}\cdot$ and $\text{HOO}\cdot$ radicals from the plasma are frozen upon the cold surface of a cryostat situated coaxially in the sample tube.

So long the quartz tube is cooled with N_2 gases flowing through liquid nitrogen (78 K), till an additive signal of $\text{HO}\cdot$ ($g_{\parallel} = 2.0450$, $g_{\perp} = 2.0089$, $a_{\text{HO}\cdot} \approx 5$ mT) and of $\text{HOO}\cdot$ ($g_{\parallel} = 2.0500$, $g_{\perp} = 2.0080$, $a_{\text{HOO}\cdot} = 1.5$ mT) is measurable (Fig. 21; *I*). The accumulation of both the radicals with time in different concentration relation, giving the final superimposed ESR signal, is the function of the mole ratio of $\text{H}\cdot$ and $\cdot\text{O}$ in the plasma. This can be regulated according to the flowing rate of H_2O vapours and of oxygen through the microwave zone. As long as the reaction proceeds in a low mole surplus of atomized oxygen



in the additive anisotropic ESR signal, the large splitting of the HO• signal from the hydrogen nucleus ($a_{\text{H}} \doteq 5 \text{ mT}$) is clearly seen (Fig. 21; 1). At further increase of O₂ concentration the HO• signal disappears and only the anisotropic signal of HOO• is dominating (Fig. 21; 2). The measured spectroscopic parameters of the frozen HO• and HOO• radicals are in good agreement with the data published [10, 20, 22—24]. Admixing H• to the plasma gases, in consequence of a surface reaction $\text{HOO}\cdot + \text{H}\cdot \rightarrow \text{HOOH}$ the ESR signal of HOO• can be stepwise erased.

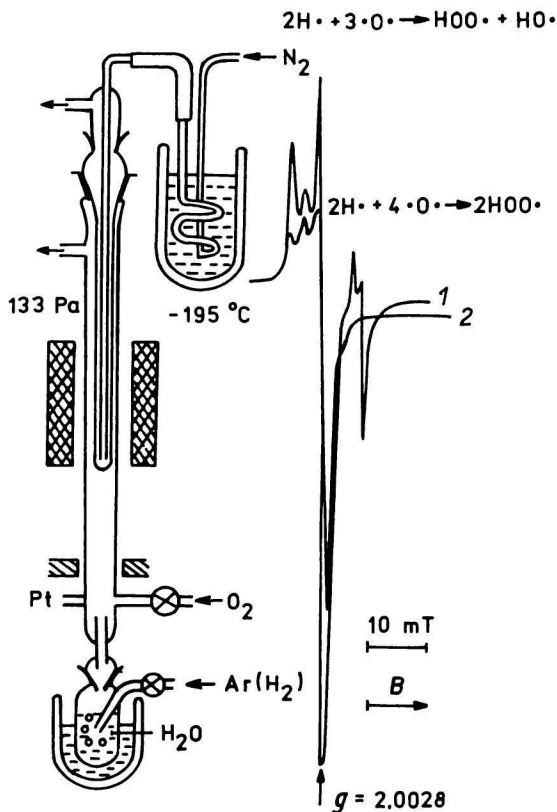
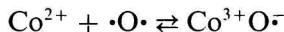


Fig. 21. Experimental arrangement for immobilization of radicals from the cold microwave plasma by freezing on the surface of the cryostat situated in the ESR cavity, and the ESR signals, when the mole ratio between the atomic hydrogen and atomic oxygen is 2:3 (1) and 1:2 (2). Experimental conditions: pressure 133 Pa and microwave power 40 W.

Reaction of atomic oxygen with solid targets at room temperature

Electron transfer from chelated transition metals

When a quartz tube centred in the ESR cavity is coated with cobalt(II) acetylacetonate evaporated from benzene solution and contacted with the stream of atomic oxygen (Fig. 22; *A*), the characteristic line of $\cdot\text{O}\cdot$ ($g = 1.5$) is not seen (Fig. 22; *B*). However, with prolonged exposure a broad signal with high g -value 2.164, characteristic of cobalt complexes with oxygen, is increasing (Fig. 22; *B*, 2, 3, 4). At a vacuum of 1.3 Pa and 24 W microwave power the increase of the line reaches after 30 min its maximum and then remains unchanged as long as the microwave radiation is in operation constantly decomposing the inlet of the molecular oxygen. When the radiation is set off and the vacuum is held constant, the broad line disappears with time (Fig. 22; *C*). With increasing power of the ESR clystron the broad line also increases but not linearly (Fig. 22; *D*) indicating a weak line saturation effect. The facts observed can be explained on the basis of assuming an equilibrium between the atomic oxygen and a paramagnetic complex Co^{3+}O^- created after the transfer of one electron from Co^{2+} ($3d^7$) to atomic oxygen contacting the surface of the crystalline layer of the $\text{Co}(\text{acac})_2$



This complex in absence of $\cdot\text{O}\cdot$ slowly decomposes in vacuum at ambient temperature. The described one-electron transfer process to atomic oxygen is similar to the reversible dioxygen binding on the surface of Co^{2+} centres of heterogeneous oxygen carriers [25]. However, the ESR parameters of the formed superoxo-adducts $\text{Co}^{3+}\text{O}_2^-$ resulting from oxygen adsorption on the surface of CoO-MgO solid solution at 77 K are different. The ESR spectrum recorded at 13 Pa is rather complex and can be assigned to slightly different paramagnetic centres characterized by apparently axial g -tensor ($g_1 = 2.120 - 2.141$, $g_3 = 1.983 - 1.990$) and hyperfine octet structure due to the ^{59}Co nucleus ($I = 7/2$, $a_3 = 1.75$ mT). Components of the signal disappear upon evaporation at room temperature but can be restored by O_2 readmission. The missing hyperfine structure in our case of the assumed Co^{3+}O^- complex can be explained by the pronounced line-broadening.

Surface reactivity with double bond of polymers

Atomic oxygen reacts immediately in contact with double bond. This is demonstrated in the course of a solid surface reaction, when the quartz target tube inserted into the ESR cavity, is covered with an evaporated film of natural rubber (NR) or polyisoprene. Without the rubber layer on the target tube the

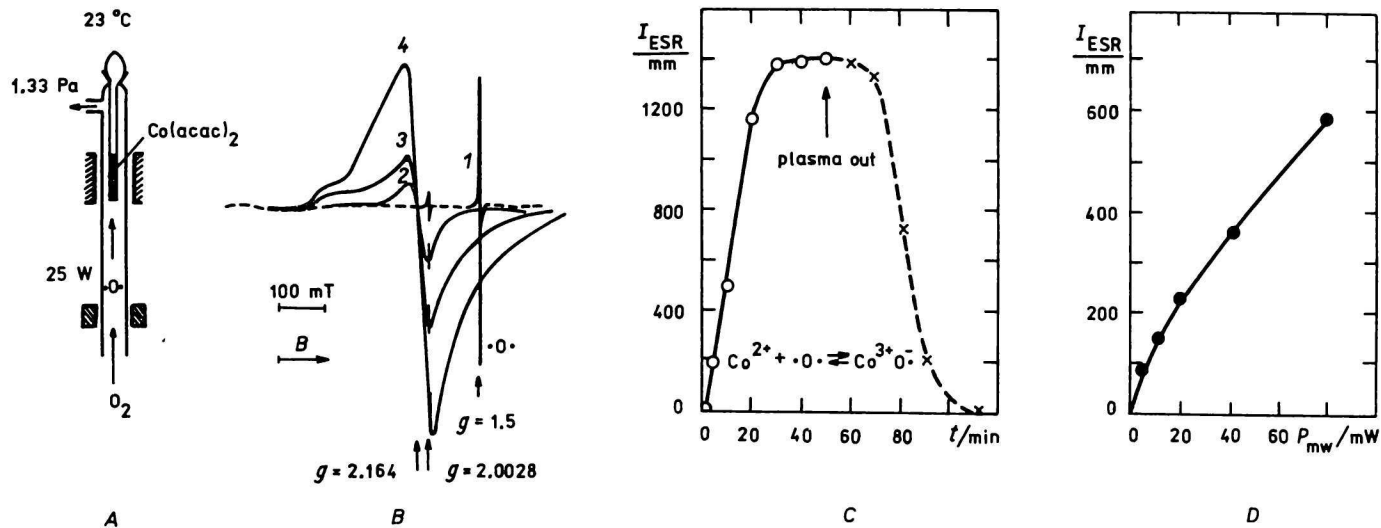


Fig. 22. *A*. Experimental arrangement for studying the attack of atomic oxygen of the crystalline $\text{Co}(\text{acac})_2$. *B*. ESR signal of atomic oxygen immediately when O_2 gas is fed into the microwave zone at 6.65 Pa (1), and stepwise generation of a broad line registered after 5 (2), 10 (3) and 30 (4) min. *C*. Dependence of the height of the broad ESR signal of $\text{Co}^{3+}\text{O}^{\cdot-}$ ($g = 2.164$) on time at 6.65 Pa. After 50 min the microwave radiation is switched off. *D*. Dependence of the intensity of the broad ESR line in arbitrary units on the applied power of the clystron.

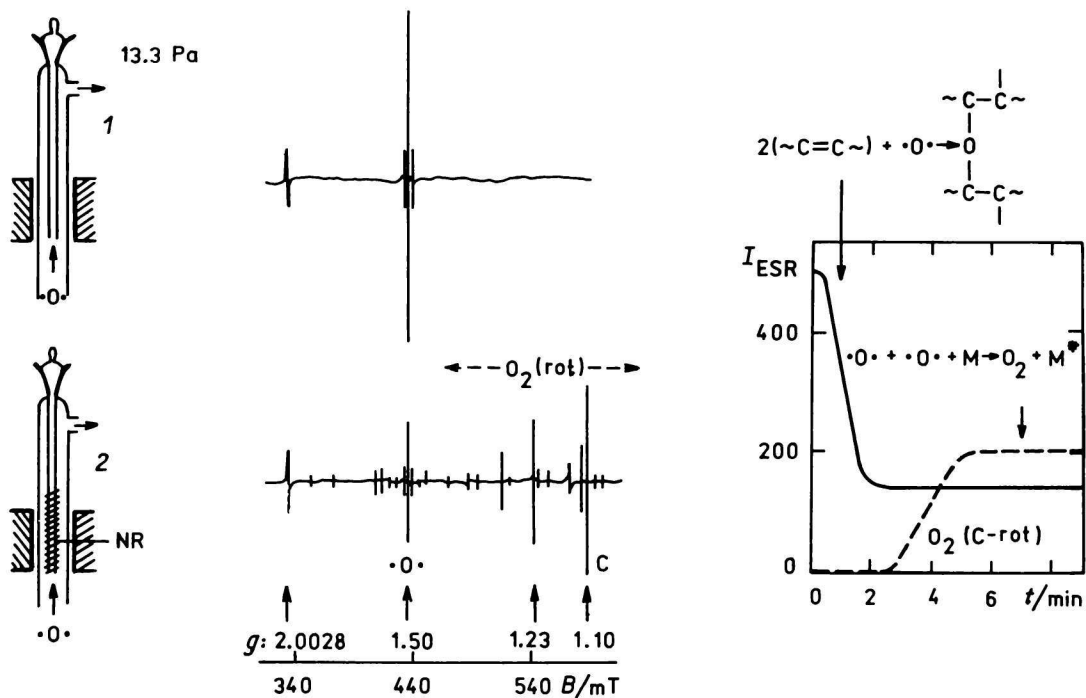


Fig. 23. Schematic experimental arrangement and ESR signal of cold microwave plasma of atomized O_2 at 13 Pa without any polymer film on the surface of the inserted quartz target tube (1), and with a film coating of evaporated natural rubber (NR) (2). Decrease of the intensity of the ESR signal of atomized oxygen ($g = 1.5$) and the increase of the C-line component of the multiline signal of molecular oxygen with time.

atomic oxygen in the cold plasma at 13.3 Pa is manifested with the nonresolved line at $g = 1.5$ (Fig. 23; 1). When the tube is coated with NR film after a short induction period of half a minute, the original intensity of the $\bullet\text{O}\bullet$ line decreases to a low level and simultaneously up to the third minute starts the increase of the multiline signal of molecular oxygen (Fig. 23; 2). The maximum of line intensities is reached after 5 min. After 20 min exposing of the NR to $\bullet\text{O}\bullet$ no mass loss was observed, but the original solubility in benzene decreases down to 60 % followed by an effective gelation.

These results are in good agreement with the systematic studies of *Golub et al.* [26—28] of the surface recession (etching) of thin films of different polymers exposed to atomic oxygen downstream from a nonequilibrium radiofrequency O_2 plasma. Indeed, cross-linked natural rubber had been reported to be much more resistant to O_2 plasma etching than the corresponding uncrosslinked polyisoprene [29]. Vinyl double bonds exert a strong protective effect in polybutadienes against surface recession (mass loss). For the polyalkenamers the etching rates increase with the decrease in $-\text{CH}=\text{CH}-$ unsaturation. When instead of natural rubber a poly(tetrafluoroethylene) (Teflon) thin tube was inserted into the ESR cavity, already from the beginning of exposition to $\bullet\text{O}\bullet$, instead of the signal of atomic oxygen with $g = 1.5$ only the multiline ESR signal of molecular oxygen as the product of the atomic oxygen recombination on the resistant Teflon surface is seen. With the prolonged exposition time and decrease of the recombination heat absorption on the Teflon surface the signal of $\bullet\text{O}\bullet$ begins to rise. Teflon coating manifested its high resistance against etching also in the space experiments as well as in laboratory as reported by *Golub et al.* [28].

The problem of the surface recession of different polymers attacked with atomic oxygen is still paid a considerable attention with the aim of seeking protective coatings for space applications [28], namely in the distance of *ca.* 230 km above the Earth's surface (Shuttle flight). The most abundant constituent of the space environment with extremely high vacuum 5×10^8 atoms/cm³ is the ground-state atomic oxygen $^3\text{P}_2$ (*ca.* 80 %) as the product of photodissociation of O_2 . With increased partial pressure of molecular oxygen by approaching the Earth's surface atomic oxygen is transformed to ozone ($\bullet\text{O}\bullet + \text{O}_2 \rightarrow \text{O}_3$).

Under influence of UV or strong local microwave radiation in the presence of humidity ozone is decomposed to atomic oxygen. This reacts with water and $\text{HO}\bullet$ radicals are formed ($\bullet\text{O}\bullet + \text{HOH} \rightarrow 2 \text{HO}\bullet$). The steady-state concentration of $\text{HO}\bullet$ radicals in the Earth's atmosphere is different during the day and night (decrease from 6×10^6 spin cm⁻³ to 6×10^5 spin cm⁻³) [30].

The combination of ESR technique with simultaneous generation of controlled concentrations of atomized gases (up to 2×10^{16} spin cm⁻³) can also help to simulate some special radical problems other than those discussed in this

paper (e.g. by HO• radicals catalyzed oxidations of NO•, •SO• to acid rain or surface attack of biological systems in environment).

Acknowledgements. The author expresses his gratitude to M. Tkáčová for her excellent help in the preparation of this manuscript, and to Dr. A. Cook from the Liverpool Polytechnic for reading the paper and useful comments.

References

1. Krongelb, S. and Strandberg, M. W. P., *J. Chem. Phys.* 31, 1196 (1950).
2. Beringer, R. and Castle, J. G., *Phys. Rev.* 81, 82 (1951).
3. Rawson, E. B. and Beringer, R., *Phys. Rev.* 88, 677 (1952).
4. Beringer, R. and Rawson, E. B., *Phys. Rev.* 87, 228 (1952).
5. Heald, N. M. A. and Beringer, R., *Phys. Rev.* 96, 645 (1954).
6. McDonald, C. C., *J. Chem. Phys.* 39, 3159 (1963).
7. Westenber, A. A. and de Haas, N., *J. Chem. Phys.* 40, 3087 (1964).
8. Westenber, A. A. and Fristrom, R. M., *Tenth Symposium (International) on Combustion*. P. 473—483. The Combustion Institute, Academic Press, New York, 1965.
9. Henry, A. F., *Phys. Rev.* 80, 396 (1950).
10. Radford, H. E., *Phys. Rev.* 122, 114 (1961).
11. Nalbandyan, A. B., *Usp. Khim.* 35, 587 (1966).
12. Ingram, D. J. E., in *Free Radicals as Studied by Electron Spin Resonance*. P. 222—227. Butterworths Scientific Publications, London, 1958.
13. Kevan, L., in *Methods in Free Radical Chemistry*, Vol. I, p. 27. (Huyer, E. S., Editor.) M. Dekker, New York, 1969.
14. Tkáč, A., *International Conference on Advances in the Stabilization and Controlled Degradation of Polymers*, V. II., p. 86—98. (Patsis, A. V., Editor.) Technomic Pub. 60, Lancaster—Basel, 1987.
15. Livingston, R., Zeldes, H., and Taylor, E. H., *Discuss. Faraday Soc.* 19, 166 (1955).
16. Broida, H. P., *Ann. Acad. Sci.* 67, 530 (1957).
17. Abragam, A. and Van Vleck, J. H., *Phys. Rev.* 92, 1448 (1953).
18. Kleinmann, I. and Polej, B., *Chem. Listy* 65, 1 (1971).
19. Adrian, F. J., *Phys. Rev.* 127, 837 (1962).
20. Carlier, M., Pauwels, F. F., and Sochet, L. R., *The Second International Specialists Meeting of the Combustion Institute on Oxidation*. Oxidation Communication, p. 1—13. Budapest, 1982.
21. Buettner, G. R., *Free Radical Biology and Medicine* 3, 259 (1987).
22. Adrian, F. J., Cochran, E. L., and Bowers, V. A., *J. Chem. Phys.* 47, 5441 (1967).
23. Shakhna Zaryan, I. K., Sachyan, G. A., Philipossyan, A. G., and Nalbandyan, A. B., *Int. J. Chem. Kinet.* 5, 693 (1974).
24. McCain, D. C. and Palke, W. E., *J. Magn. Reson.* 20, 52 (1975).
25. Che, M., Dyrek, K., Giamello, E., and Sojka, Z., *Z. Phys. Chem. (München)* 152, 139 (1987).
26. Golub, M. A. and Wydeven, T., *Polym. Degrad. Stab.* 22, 325 (1988).
27. Golub, M. A., Wydeven, T., and Cormia, R. D., *Polymer* 30, 1571 (1989).
28. Wydeven, T., Golub, M. A., and Lerner, N. R., *J. Appl. Polym. Sci.* 37, 3343 (1989).
29. Hansen, R. H., Pascale, J. V., De Benedicts, T., and Rentzepis, P. M., *J. Polym. Sci., A* 3, 2205 (1965).
30. Ehhalt, D. H., *Free Rad. Res. Commun.* 3, 153 (1987).

Translated by A. Tkáč